RESEARCH ARTICLE

Check for updates

A turn-off fluorescent probe for the detection of Cu²⁺ based on a tetraphenylethylene-functionalized salicylaldehyde Schiff-base†

Hai-Fang Xie,[a] Chang-Jin Yu,[b] Ya-Li Huang,[c] Hong Xu,*[c] Qi-Long Zhang,*[c] Xiao-Hong Sun,[d] Xing Feng [ID] *[e] and Carl Redshaw [ID] [f]

A non-planar tetraphenylethylene-functionalized salicylaldehyde Schiff-base fluorescent probe (**TPE-An-Py**) with aggregation-induced enhanced emission (AIEE) characteristics was synthesized *via* a classical Knoevenagel condensation reaction, and exhibited a high sensitivity towards copper ions in aqueous media with a "turn-off" fluorescence mechanism; the limit of detection is 2.36×10^{-7} mol L^{-1}. Importantly, the coordination mode of the probe towards copper was further evaluated by UV-vis and NMR spectroscopy and a $1:2$ stoichiometry was identified. A single crystal X-ray diffraction study confirmed the binding mode. In addition, the AIEE fluorescent probe can be applied to the detection of Cu²⁺ in practical samples with satisfactory recoveries in a range of 106–111% in lake water and 97–108% in tap water.

Introduction

Copper, a group 11 transition element, is an abundant, inexpensive and naturally occurring metal which has been widely utilized as a raw material for the preparation of common tools for over 5000 years.[1] Currently, copper is a major industrial metal, ranking number three in terms of quantities consumed.[2] On the other hand, copper is an essential trace element in the human body, and plays a significant role in maintaining the central nervous system, cardiovascular system and hematopoietic function, as well as regulating the physiological activity of enzymes.[3–6] An excessive or lack of copper in the body can lead to significant health problems, such as Alzheimer's disease, Parkinson's disease and ALS.[7–10]

The industrial revolution has led to serious environment problems, involving atmospheric, water and soil pollution. One example is copper pollution of water which can lead to risks to human health.[11] Thus, the monitoring and selective detection of copper ions has become a highly relevant research topic for environmental scientists.

Fluorescent methods are a wonderful tool for Cu²⁺ detection due to their simplicity, fast response and high detection limits, and have been applied in the fields of life science, food and environmental science.[12–15] However, most of the conventional fluorophores with π-conjugation suffer from aggregation-caused quenching (ACQ) in condensed media resulting in a low fluorescence quantum yield, which limits their high-technological application.[16–18] The disadvantages associated with the ACQ effect were solved by Tang in 2001, who innovatively designed aggregation-induced emission luminogens (AIEgens) that exhibited negligible emission in solution, but enhanced emission in the solid state. A mechanism involving restriction of intra-molecular motion (RIM) was proposed to clarify the abnormal photo-physical phenomenon.[19] Following on from this mechanism, a large number of AIEgens have been synthesized for potential application in organic electronics, chemsensors, boilable, *etc.*

On the other hand, excited-state intramolecular proton transfer (ESIPT)[20] is a fantastic fluorescence process that exhibits a uniquely large Stokes shift with AIE characteristics, arising from the active hydrogen of a phenolic hydroxyl which can easily transfer from the enol form to the keto form *via* a photo-tautomerization process under photoexcitation. Moreover, the process is very fast on the sub-picosecond time scale in the

[a] *School of Public Health, The Key Laboratory of Environmental Pollution Monitoring and Disease Control, Ministry of Education, Guizhou Medical University, Guiyang 550025, China*

[b] *School of Biology and Engineering, Guizhou Medical University, Guiyang, 550025, China*

[c] *School of Basic Medical Sciences, Guizhou Medical University, Guiyang 550025, China. E-mail: gzuqlzhang@126.com, xuhong@gmc.edu.cn*

[d] *School of Food Safety, Guizhou Medical University, Guiyang 550025, China*

[e] *Guangdong Provincial Key Laboratory of Functional Soft Condensed Matter, School of Material and Energy, Guangdong University of Technology, Guangzhou 510006, P. R. China. E-mail: hyxhn@sina.com*

[f] *Department of Chemistry & Biochemistry, University of Hull, Cottingham Road, Hull, Yorkshire HU6 7RX, UK*

† Electronic supplementary information (ESI) available: ¹H/¹³C NMR spectra and the absorption spectra of probe, *etc.* CCDC 1967709 and 1967696. For ESI and crystallographic data in CIF or other electronic format see DOI: 10.1039/c9qm00759h

1500 | *Mater. Chem. Front.*, 2020, **4**, 1500–1506

This journal is © The Royal Society of Chemistry and the Chinese Chemical Society 2020

excited state.[21–24] For example, 4-N,N-dimethylaminoaniline salicylaldehyde (DAS) displays a typical ESIPT process with an obvious AIE feature, which exhibits yellow emission (530 nm) in the aggregation state, but is not emissive in solution.[25] Up to now, few examples of Cu^{2+} detection based on an ESIPT system have been reported.[26,27]

In this contribution, we have developed a novel fluorescence probe possessing AIE plus ESIPT characteristics (**TPE-An-Py**), which exhibits high specificity and selectivity for the detection of copper(II) in a water environment with a limit of detection as low as 2.36×10^{-7} mol L^{-1}. The detection mechanism was investigated by ^1H NMR spectroscopic titrations and by single crystal X-ray diffraction. Furthermore, the probe can be utilized for the detection of Cu^{2+} in real water samples. This article provides a new strategy for extending the practical applications of AIEgens in the environmental field.

Results and discussion

Synthesis and characterization of the target compound TPE-An-Py

The target compound **TPE-An-Py** was synthesized as presented in Scheme 1. A Knoevenagel condensation reaction between 2-hydroxy-5-(1,2,2-triphenylvinyl)-benzaldehyde (**1**) and pyridine-2,6-dicarboxamide in methanol afforded the target compound in 60% yield. The molecular structure was characterized by $^1H/^{13}C$ NMR spectroscopy, HRMS, as well as by single crystal X-ray diffraction (Fig. S1–S4, ESI†).

X-Ray single crystal diffraction analysis

Fortunately, single crystals of the chromophore **TPE-An-Py** suitable for X-ray diffraction were cultivated from a mixture of $CHCl_3$ and methanol by slow evaporation, and the crystal structure refinement parameters are summarized in Table S1 (ESI†). The crystal belongs to the triclinic system with the space group $P\bar{1}$, and an asymmetric unit containing one molecule of **TPE-An-Py** with two $CHCl_3$ solvent molecules. As shown in Fig. 1, the structure of the fluorescence dye **TPE-An-Py** possesses a bridging pyridyl unit that adopts a twisted molecular conformation with a twist angle of 29.8°, and the two terminal TPE units which overlap with each other and formed a helical conformation;[28] several weak O–H···N interactions (O2–H2A···N4 = 1.882 Å, O3–H3···N5 = 1.858 Å) and N–H···O interactions (N1–H1···O2 = 2.344 Å, N23–H2···O3 = 2.394 Å) were observed. Moreover, a crown-like ether ring with a diameter

Fig. 1 The X-ray structure of **TPE-An-Py** (A) front view and (B) side view.

of ∼4.5 Å was formed by the self-assembly of the bridge unit and two TPE moieties (Fig. 1).

AIE properties

The fluorescent dye **TPE-An-Py** exhibits good solubility in common solvents, such as dichloromethane (CH_2Cl_2), tetrahydrofuran (THF), N,N-dimethylformamide (DMF) and 1,4-dioxane, but is insoluble in water. Tetraphenylethylene (TPE) is a typical AIE luminogen, thus to investigate the AIE properties of the Schiff-base **TPE-An-Py**, the emission behaviour in dilute THF and THF/water mixtures was measured and are listed in Fig. 2. The **TPE-An-Py** displays weak red emission in pure THF with a maximum emission peak ($\lambda_{max\,em}$) at 598 nm, originating from the keto peak, while the emission peak with low intensity at 477 nm corresponds to the enol peak. As the water fraction (f_w) gradually increases from 0% to 60%, the fluorescence intensity is slightly quenched which may arise from a contribution to the intramolecular charge transfer (ICT) with the increase of the
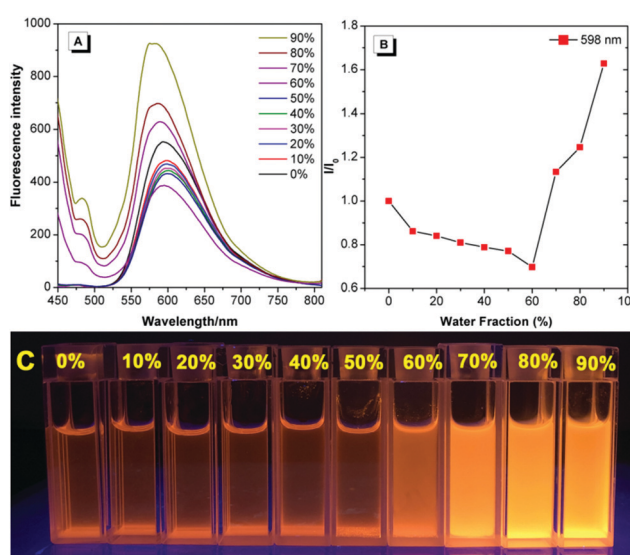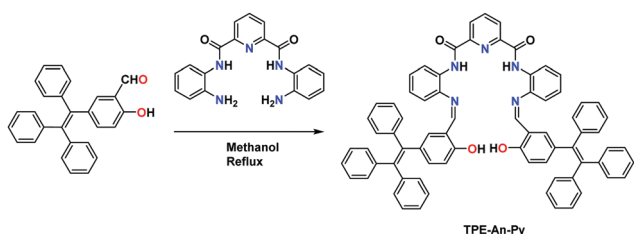

Fig. 2 (A) Fluorescence spectra of **TPE-An-Py** (1.00×10^{-4} mol L^{-1}) in THF/water mixtures with different water fractions (λ_{ex} = 415 nm, slit: 5/5 nm, voltage: 900 V). (B) Plots of I/I_0 values *versus* the compositions of THF/water mixtures, in which I_0 is the PL intensity in pure THF solution. (C) photographs in THF/water mixtures with different water fractions taken under 365 nm UV irradiation.

Scheme 1 Synthetic route to probe **TPE-An-Py**.

This journal is © The Royal Society of Chemistry and the Chinese Chemical Society 2020

Mater. Chem. Front., 2020, **4**, 1500–1506 | **1501**

polarity of the solvent. On increasing the f_w above 60%, the emission intensity was enhanced dramatically, and an approximate 2-fold enhancement at $f_w = 90\%$ compared to when in THF was observed. The maximum emission peak was located at 575 nm, corresponding to the keto peak. In addition, the quantum yield in the solid state ($\Phi_f = 18.1\%$) is higher than that compared to when in THF solution ($\Phi_f = 9.5\%$). Thus, the fluorescent dye **TPE-An-Py** is AIEE-active. The fluorescence spectrum for **TPE-An-Py** in the solid state was also measured and possessed a maximum emission peak at 711 nm, which may be due to the synergistic effect of the classical ESIPT process and a twisted intramolecular charge transfer process, and the possible keto-hydroxyl tautomerism structure is presented in Fig. S6 (ESI†).

Detection experiments

Schiff-based compounds are excellent ligands to coordinate with metal ions (such as rare-earth metals, transition metals, alkali metals and alkali earth metals) with potential applications in organic catalysis,[29–32] and also have been widely explored as chemisensors for the detection of metal ions, due to their high binding affinity.[33,34] Herein, to test the detecting ability of the TPE-functionalized Schiff-base **TPE-An-Py**, the probe (1.00×10^{-4} mol L^{-1}) with various cations (such as Cd^{2+}, Cu^{2+}, K^+, Pb^{2+}, Li^+, Fe^{3+}, Ca^{2+}, Mg^{2+}, Co^{2+}, Cr^{3+}, Al^{3+}, Ba^{2+}, Ni^{2+}, Zn^{2+}, Ag^+, Na^+, Hg^+, $[M]^{n+} = 2.00 \times 10^{-4}$ mol L^{-1}) was evaluated in mixtures of THF and water ($V_{THF}/V_{water} = 4/1$, pH = 7.00). The UV-vis absorption spectroscopy indicated that the absorption peak at 439 nm was enhanced on addition of Cu^{2+} to the solution containing the probe **TPE-An-Py**, while other metal ions only showed a limited effect on the absorption behaviour. However, the colour of the solution changed from colourless to yellow in the presence of Cu^{2+} and Fe^{3+} under sunlight, indicating that the probe **TPE-An-Py** coordinates with copper(II) and iron(III). On the other hand, the fluorescence spectra revealed that the fluorescence intensity of the probe ($\lambda_{em\,max} = 598$ nm) was quenched by ca. 2-fold in the presence of either Cu^{2+} and Fe^{3+} compared to a blank solution (Fig. 3). It is noteworthy that other metal ions had a limited effect on the fluorescence behaviour, indicating that the TPE-based Schiff-base **TPE-An-Py** can be used as a fluorescent probe for sensing Cu^{2+}, but that the iron(III) may be a key interference ion when for probing Cu^{2+}.

Optimization of experimental conditions

Schiff-based compounds are known to undergo a hydrolysis reaction in either strong acid or alkali solution. Thus, the stability of probe **TPE-An-Py** was investigated at various pH values from 2.00–11.00. In the presence of Tris–HCl buffer, tetrahydrofuran/water mixtures ($V_{THF}/V_{water} = 4/1$) with pH values over the range 2.00 to 11.00 were prepared for testing. As shown in Fig. S7 (ESI†), upon excitation, the fluorescence behaviour of probe **TPE-An-Py** remains relatively unchanged as the pH value increases from 2.00 to 11.00, which indicates that the Schiff base probe is stable. On the other hand, to evaluate the coordination reaction time between the probe and copper(II), as the Cu^{2+} is added, the fluorescence intensity

Fig. 3 (A) The UV-vis and (B) fluorescence spectra of the fluorescence probe **TPE-An-Py** (1.00×10^{-4} mol L^{-1}, $V_{THF}: V_{H_2O} = 4/1$, Tris–HCl buffer 2.00×10^{-3} mol L^{-1}, pH = 7.00) interacting with different metal ions (2.00×10^{-4} mol L^{-1}) ($\lambda_{ex}/\lambda_{em} = 415/598$ nm, slit: 5/5 nm, voltage: 900 V). (C) Photograph of **TPE-An-Py** interacting with metal ions under natural light and (D) under a 365 nm UV lamp.

gradually decreased until a balance was reached within 15 min (Fig. S8, ESI†). Thus, in order to simulate a natural water environment for further experiments, all of the sensing properties of the probe were carried out at pH = 7.00 using Tris–HCl buffer solution after 20 min (Fig. S9, ESI†).

Based on the optimized experimental conditions, the fluorescence titration experiments were performed with progressive addition of Cu^{2+} and are presented in Fig. 4. The fluorescence intensity of probe **TPE-An-Py** at $\lambda_{max\,em} = 598$ nm gradually decreased as the Cu^{2+} ion was added. The binding constant for the Cu^{2+} ion was estimated to be 3.3388×10^3 M^{-1} in THF/water ($V_{THF}/V_{water} = 4/1$) (Fig. S12, ESI†). Furthermore, the detection limit was calculated from the fluorescence titration experiments following the IUPAC method (Fig. 4). Ten groups of blank experiments were performed in the absence of Cu^{2+} under the same conditions, and the fluorescence value at

Fig. 4 (A) Fluorescence spectra on addition of Cu^{2+} to the probe (1.00×10^{-4} mol L^{-1}, $V_{THF}: V_{H_2O} = 4/1$, $\lambda_{ex} = 415$ nm, slit: 5/5 nm, voltage: 900 V). (B) Linear fitting of the emission data upon addition of Cu^{2+}.

1502 | *Mater. Chem. Front.*, 2020, **4**, 1500–1506

This journal is © The Royal Society of Chemistry and the Chinese Chemical Society 2020

the wavelength of 598 nm was taken for the standard deviation (SD) calculation. The emission intensity of probe **TPE-An-Py** at 598 nm was then plotted against the concentration of Cu^{2+}. According to the formula: detection limitation = 3SD/S, a linear relationship in the range of 5.00×10^{-6} mol L^{-1} to 1.20×10^{-4} was observed with R^2 = 0.99294, and the limit of detection (LOD) is 2.36×10^{-7} mol L^{-1}. The low LOD indicates that the probe is an excellent chemisensor for Cu^{2+}.

Furthermore, to investigate the selectivity of the probe toward Cu^{2+}, a selection of both cations and anions were added as potential interfering coexisting ions. Firstly, to the solutions of **TPE-An-Py** and Cu^{2+} were added 10 equiv. of various metal ions (such as Li^+, Na^+, K^+, Mg^{2+}, Ca^{2+}, Ba^{2+}, Al^{3+}, Fe^{3+}, Co^{2+}, Ni^{2+}, Zn^{2+}, Cr^{3+}, Pb^{2+}, Cd^{2+}, Hg^{2+}, Ag^+) and anions (AcO^-, F^-, CO_3^{2-}, SO_3^{2-}, HSO_3^-, Cl^-, SO_4^{2-}, NO_2^-, Br^-, I^-). In the presence of Cu^{2+}, the emission intensity of the mixture at λ_{em} = 598 nm was quenched, while without Cu^{2+}, the emission barely changed, which suggested that the coexisting ions and anions had a limited effect on the detection of Cu^{2+}. Thus, the interference experiments indicated that the probe displays high specificity and selectivity for the detection of the Cu^{2+} ion (Fig. 5 and Fig. S13, ESI†). By contrast, in the presence of Fe^{3+}, the colour of the solution containing **probe@Cu²⁺@Fe³⁺** clearly became dark by naked-eye detection, and this is attributed to the iron(III) as the main interference ion. Thus, Fe^{3+} plays a significant role in affecting the probes detection of Cu(II) in solution (Fig. S9, ESI†).

In addition, the effect of pH value on the detection of Cu^{2+} ions was also investigated. As shown in Fig. S10 (ESI†), the fluorescence intensity of the **TPE-An-Py@Cu²⁺** at 598 nm show a limited change over a broad pH range from 2.00–11.00, indicating that the **TPE-An-Py** is a stable fluorescent probe for detecting Cu^{2+} in acid–base environments and is suitable for practical applications.

A possible mechanism for detecting Cu^{2+}

We previously reported that a similar Schiff-base can coordinate with Cu^{2+} in a 1:2 stoichiometric ratio, and that the copper centre was coordinated *via* the N and O atoms in a dinuclear complex.[35] In order to further analyze the binding mechanism of probe **TPE-An-Py** with Cu^{2+}, the mole-ratio method and a Job's plot were carried out to elucidate the stoichiometry; a 1:2 complexation of **probe@Cu²⁺** was confirmed (Fig. S11–S13, ESI†). Information on
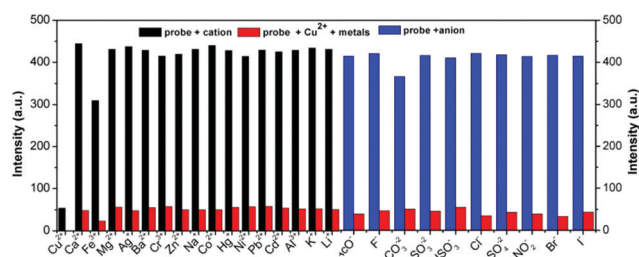
the binding properties of the probe with Cu^{2+} was obtained from ^{1}H NMR spectroscopic titration experiments in d-DMSO : D_2O solution (5:1, v/v). For the probe, three singlets (δ = 13.43, 10.48 and 7.87 ppm) were observed for –OH, –C–NH–C=O and –CH=N–, respectively, two doublets (δ = 8.48) and a triplet (δ = 8.39–8.33) for the pyridine and diphenylamine ring, respectively. The protons at δ = 8.06 and 7.07–7.29 ppm are from the TPE units and the signal at δ = 5.70 ppm originated from the diphenylamine ring. Upon gradual addition of Cu^{2+} (0.1 equiv.) to the probe solution, the proton signal at δ 13.43 (–OH) disappeared, consistent with initial Cu^{2+} coordination at the O atom of the hydroxyl group. On continuously adding Cu^{2+} (0.3 equiv.), all protons signals in the region of 7.38–13.43 ppm slowly decreased, and then disappeared, when the [Cu^{2+}] reached 0.4 equiv. This suggested that the N atoms from the pyridine and diphenylamine units and the –O atom were linked with the Cu centre. All the resonances of the proton signals in the region δ = 6.8–7.2 ppm were somewhat broad and overlapped, which could be attributed to the paramagnetism of the copper centre (Fig. 6). In addition, no significant chemical shift changes were observed either before or after adding the Cu^{2+}.

Fortunately, crystals of the complex **probe@Cu²⁺** were cultivated by slowly evaporating a solution of methanol/CH_2Cl_2. The complex crystallizes in the triclinic space group $P\bar{1}$. The X-ray crystal structure of **probe@Cu²⁺** shows that Cu1 adopts a five-coordinate geometry with three N atoms (N1, N2 and N3) and one O (O2) from the ligand and one O (O5) from methanol, while Cu2 is four-coordinate, being bound to two nitrogen atoms (N4 and N5) and two oxygen (O1 and O1′). Importantly, the bridge Cu2–O1 bond (1.989 Å) plays a significant role in binding two ligands to form a 3D stacking structure along the a axis. As expected, the ligand coordinates with two Cu(II) ions consistent with the mole-ratio method described earlier and in the experimental (Fig. 7).

To gain insight and evaluate the potential application of probe **TPE-An-Py** for detecting Cu^{2+} in environmental water, water samples containing trace amounts of Cu^{2+} were collected
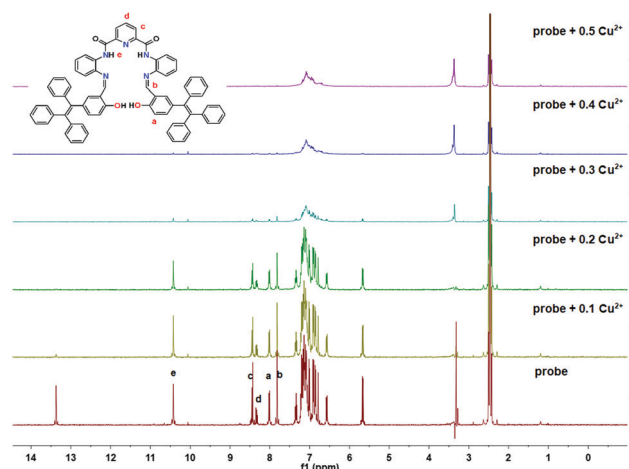

Fig. 5 Bar diagram of the competitive experiments of various metal cations and anions on the fluorescence intensity of the probe/Cu^{2+} complex in buffer solution ($\lambda_{ex}/\lambda_{em}$ = 415/598 nm, slit: 5/5 nm, voltage: 900 V).

Fig. 6 ^{1}H NMR spectroscopic titration spectra of **probe@Cu²⁺** on increasing concentrations of Cu^{2+} in d-DMSO solution.
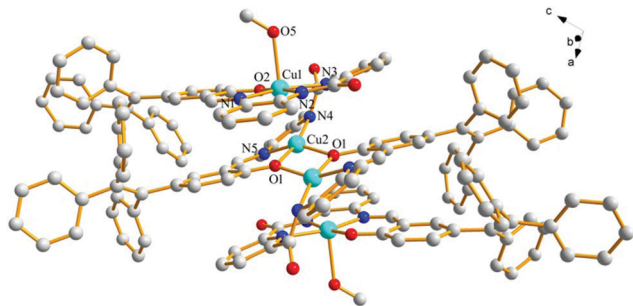
Fig. 7 The crystal of complex **probe@Cu^{2+}**, the hydrogen atom are omitted for clarity.

Table 1 Detection of Cu^{2+} in water samples

Sample	Measured (μmol L^{-1})	Added (μmol L^{-1})	Detected (μmol L^{-1})	Recovery (n = 3, %)	RSD (%)
Artificial lake	13.33	21	36.68	111	1.2
		80	99.05	107	1.4
		160	184.08	106	2.4
Running water	8.93	21	29.17	97	1.9
		80	91.34	103	3.6
		160	180.93	108	2.0

from both the lake (at Medical University of Guizhou Medical University) and tap water (laboratory) and were filtered for further testing. The fluorescence intensity of probe **TPE-An-Py** exhibited a remarkable emission intensity quenching at 598 nm accompanied by a colour change from bright to dark under UV irradiation (λ_{ex} = 365 nm). The recoveries were calculated in the range 106–111% for lake water and 97–108% in tap water for Cu^{2+}. Thus, the high selectivity and specificity of the probe **TPE-An-Py** means it could be used for monitoring Cu^{2+} in a water environment.

Conclusions

In conclusion, we present a novel "turn-off" type AIEE fluorescence probe containing a pyridine-2,6-dicarboxamide core and two TPE moieties linked *via* a phenylenediamine bridge, which acts as a selective sensor for copper(II) in THF/water mixtures, as well as in real water samples. Also the probe offers a convenient "naked-eye" detection method for Cu(II) ion detection and the detection limit is as low as 2.36×10^{-7} mol L^{-1}. UV-vis and NMR spectra shows that the probe adopts a 1:2 binding mode with the copper centre, with a binding constant of 3.3388×10^{3} mol L^{-1}, and the result is agreement with the single crystal X-ray diffraction analysis. We believe our research provides an example of an AIEgen probe for Cu(II) detection in practical applications, and moreover, the basic molecular framework of the ligand can be further functionalized to make it specific for other analytes. Such studies are currently on-going in our laboratory.

Experimental

General

^{1}H and ^{13}C NMR spectra (400 MHz) were recorded on a Inova-400 Bruker AV 400 spectrometer using chloroform-d solvent and tetramethylsilane as the internal reference. *J*-values are given in Hz. High-resolution mass spectra (HRMS) were taken on a GCT premier CAB048 mass spectrometer operating in a MALDI-TOF mode. UV-vis absorption spectra were obtained on a UV-2600 Milton Ray Spectrofluorometer. PL spectra were recorded on a Cary eclipse Hitachi 4500 spectrofluorometer.

Scanning electron microscopy (SEM) images were obtained using a Hitachi scanning electron microscope.

X-ray crystallography

Crystallographic data for **TPE-An-Py** were collected on a Bruker APEX 2 CCD diffractometer with graphite-monochromated Mo Kα radiation (λ = 0.71073 Å) in the ω scan mode.[36] The structures were solved by a charge flipping algorithm and refined by full-matrix least-squares methods on F^2.[37,38] All esds were estimated using the full covariance matrix. Further details are presented in Table 1. Data for the structures reported here have been deposited with the Cambridge Crystallographic Data Centre with deposition numbers CCDC 1967709 and 1967696, which contain the supplementary crystallographic data for this paper.†

Materials

Unless otherwise stated, all reagents were purchased from commercial sources and used without further purification. Tetrahydrofuran and demineralized water were distilled prior to use.

Synthesis of TPE-An-Py

A mixture of *N*,*N'*-(2-aminophenyl)-2,6-diformyl iminopyridine[39] (78.1 mg, 0.25 mmol) and 2-hydroxy-5-(1,2,2-triphenylethenyl)-benzaldehyde (188 mg, 0.50 mmol) in 50 mL anhydrous methanol solution was stirred for 4 h at room temperature. The solution changed to yellow with formation of a yellow precipitate. Then the mixture was filtered and washed with methanol three times. The yellow residue was further crystallized using THF and hexane to give yellow block crystals (160 mg, yield 60%). ^{1}H NMR (400 MHz, d-DMSO) δ 13.43 (s, 2H), 10.48 (s, 2H), 8.48 (d, J = 7.7 Hz, 2H), 8.39–8.33 (m, 1H), 8.06 (d, J = 7.9 Hz, 2H), 7.87 (s, 2H), 7.38 (t, J = 7.6 Hz, 2H), 7.29–7.07 (m, 26H), 7.05 (d, J = 7.3 Hz, 4H), 6.95 (d, J = 6.6 Hz, 4H), 6.89 (d, J = 6.5 Hz, 4H), 6.84 (d, J = 1.7 Hz, 4H), 6.61 (dd, J = 8.5, 1.9 Hz, 4H), 5.70 (d, J = 8.5 Hz, 4H). ^{13}C NMR (101 MHz, d-DMSO) δ 162.09, 161.52, 159.02, 151.64, 149.31, 147.91, 143.75, 143.60, 141.91, 140.95, 139.96, 139.78, 139.62, 135.92, 134.84, 134.22, 133.27, 131.81, 131.28, 131.10, 131.03, 128.64, 128.59, 128.37, 128.23, 127.21, MALDI-TOF-MS: *m/z* calculated for C$_{73}$H$_{53}$N$_5$O$_4$: 1063.41, obtained 1064.4172 [M + H]$^+$.

General procedure for fluorescence studies

Stock solutions (2.0×10^{-4} mol L^{-1}) of the metal ion and anion were prepared in THF. The probe **TPE-An-Py** (1.0×10^{-4} mol L^{-1}) was dissolved in THF. The excitation wavelength was 415 nm.

1504 | *Mater. Chem. Front.*, 2020, **4**, 1500–1506

This journal is © The Royal Society of Chemistry and the Chinese Chemical Society 2020

The probe **TPE-An-Py** (1.0×10^{-4} mol L^{-1}, 500 μL) in THF solution was added in to the 500 μL real water sample, then Tris–HCl (2.0×10^{-3} mol L^{-1}, pH = 7.00) buffer solution and tetrahydrofuran (3.5 mL) were added, and the mixture was left standing for 20 min before using.

Conflicts of interest

There are no conflicts to declare.

Acknowledgements

Notes and references

1 D. P. Pompeani, M. B. Abbott, B. A. Steinman and D. J. Bain, Lake Sediments Record Prehistoric Lead Pollution Related to Early Copper Production in North America, *Environ. Sci. Technol.*, 2013, **47**, 5545–5552.

2 S. Glöser, M. Soulier and L. A. Tercero Espinoza, Dynamic Analysis of Global Copper Flows. Global Stocks, Postconsumer Material Flows, Recycling Indicators, and Uncertainty Evaluation, *Environ. Sci. Technol.*, 2013, **47**, 6564–6572.

3 N. C. Andrews, Metal transporters and disease, *Curr. Opin. Chem. Biol.*, 2002, **6**, 181–186.

4 J. Chen, G. G. Ying and W. J. Deng, Antibiotic Residues in Food: Extraction, Analysis, and Human Health Concerns, *J. Agric. Food Chem.*, 2019, **67**, 7569–7586.

5 J. R. Prohaska, Impact of copper limitation on expression and function of multicopper oxidases (ferroxidases), *Adv. Nutr.*, 2011, **2**, 89–95.

6 M. C. Linder and M. Hazegh-Azam, Copper biochemistry and molecular biology, *Am. J. Clin. Nutr.*, 1996, **63**, 797S–811S.

7 H. J. Lee, K. J. Korshavn, A. Kochi, J. S. Derricka and M. H. Lim, Cholesterol and metal ions in Alzheimer's disease, *Chem. Soc. Rev.*, 2014, **43**, 6672–6682.

8 E. Gaggelli, H. Kozlowski, D. Valensin and G. Valensin, Copper homeostasis and neurodegenerative disorders (Alzheimer's, prion, and Parkinson's diseases and amyotrophic lateral sclerosis), *Chem. Rev.*, 2006, **106**, 1995–2044.

9 J. Zou, X. Wang, L. Zhang and J. K. Wang, Iron nanoparticles significantly affect the *in vitro* and *in vivo* expression of Id genes, *Chem. Res. Toxicol.*, 2015, **28**, 373–383.

10 K. N. Raymond, E. A. Dertz and S. S. Kim, Enterobactin: an archetype for microbial iron transport, *Proc. Natl. Acad. Sci. U. S. A.*, 2003, **100**, 3584–3588.

11 S. P. Hinge, M. S. Orpe, K. V. Sathe, G. D. Tikhe, N. S. Pandey, K. N. Bawankar, M. V. Bagal, A. V. Mohod and P. R. Gogate, Combined removal of Rhodamine B and Rhodamine 6G from wastewater using novel treatment approaches based on ultrasonic and ultraviolet irradiations, *Desalin. Water Treat.*, 2016, **57**, 1–13.

12 S. Wang, N. Li, W. Pan and B. Tang, Advances in functional fluorescent and luminescent probes for imaging intracellular small-molecule reactive species, *TrAC, Trends Anal. Chem.*, 2012, **39**, 3–37.

13 Y. Yang, Q. Zhao, W. Feng and F. Y. Li, Luminescent chemodosimeters for bioimaging, *Chem. Rev.*, 2013, **113**, 192–270.

14 A. W. Czarnik, Fluorescent Chemosensors for Ion and Molecule Recognition, *Instrum. Sci. Technol.*, 1994, **22**, 405–406.

15 F. Lv, X. Feng, H. Tang, L. Liu, Q. Yang and S. Wang, Development of Film Sensors Based on Conjugated Polymers for Copper(II) Ion Detection, *Adv. Funct. Mater.*, 2011, **21**, 845–850.

16 J. Luo, Z. Xie, J. W. Y. Lam, L. Cheng, H. Chen, C. Qiu, H. S. Kwok, X. Zhan, Y. Liu, D. Zhu and B. Z. Tang, Aggregation-induced emission of 1-methyl-1,2,3,4,5-pentaphenylsilole, *Chem. Commun.*, 2001, 1740–1741.

17 D. Ding, K. Li, B. Liu and B. Z. Tang, Bioprobes Based on AIE Fluorogens, *Acc. Chem. Res.*, 2013, **46**, 2441–2453.

18 C. Zhu, R. T. K. Kwok, J. W. Y. Lam and B. Z. Tang, Aggregation-Induced Emission: A Trailblazing Journey to the Field of Biomedicine, *ACS Appl. Bio Mater.*, 2018, **1**, 1768–1769.

19 J. Mei, N. L. C. Leung, R. T. K. Kwok, J. W. Y. Lam and B. Z. Tang, Aggregation-Induced Emission: Together We Shine, United We Soar!, *Chem. Rev.*, 2015, **115**, 11718–11940.

20 K. C. Tang, M. J. Chang, T. Y. Lin, H. A. Pan, T. C. Fang, K. Y. Chen, W. Y. Hung, Y. H. Hsu and P. T. Chou, Fine Tuning the Energetics of Excited-State Intramolecular Proton Transfer (ESIPT): White Light Generation in A Single ESIPT System, *J. Am. Chem. Soc.*, 2011, **133**, 17738–17745.

21 N. P. Ernsting, A. Mordzinski and B. Dick, Excited-state intramolecular proton transfer in jet-cooled 2,5-bis(2-benzothiazolyl)-hydroquinone, *J. Phys. Chem.*, 1987, **91**, 1404–1407.

22 J. Zhang, S. Ma, H. Fang, B. Xu, H. Sun, I. Chan and W. Tian, Insights into the origin of aggregation enhanced emission of 9,10-distyrylanthracene derivatives, *Mater. Chem. Front.*, 2017, **1**, 1422–1429.

23 (*a*) N. Kwon, Y. Hu and J. Yoon, Fluorescent Chemosensors for Various Analytes Including Reactive Oxygen Species, Biothiol, Metal Ions, and Toxic Gases, *ACS Omega*, 2018, **3**, 13731–13751; (*b*) Z. Hu, H. Zhang, Y. Chen, Q. Wang, M. R. J. Elsegood, S. J. Teat, X. Feng, M. M. Islam, F. Wu and B. Z. Tang, Tetraphenylethylene-based color-tunable AIE-ESIPT chromophores, *Dyes Pigm.*, 2020, **175**, 108175.

24 A. P. Demchenko, V. I. Tomin and P.-T. Chou, Breaking the Kasha Rule for More Efficient Photochemistry, *Chem. Rev.*, 2017, **117**, 13353–13381.

25 Q. Feng, Y. Y. Li, L. L. Wang, C. Li, J. M. Wang, Y. Y. Liu, K. Li and H. W. Hou, Multiple-color aggregation-induced emission (AIE) molecules as chemodosimeters for pH sensing, *Chem. Commun.*, 2016, **52**, 3123–3126.

26 D. Maity, V. Kumar and T. Govindaraju, Reactive Probes for Ratiometric Detection of Co²⁺ and Cu⁺ Based on Excited-State Intramolecular Proton Transfer Mechanism, *Org. Lett.*, 2012, **14**, 6008–6011.

27 J. W. Xiong, Z. Z. Li, J. H. Tan, S. M. Ji, J. W. Sun, X. W. Li and Y. P. Huo, Two new quinoline-based regenerable fluorescent probes with AIE characteristics for selective recognition of Cu²⁺ in aqueous solution and test strips, *Analyst*, 2018, **143**, 4870–4886.

28 R. Kumar, S. Semwal, J. Choudhury and A. Srivastava, Heli(aza)cene: A Helical Molecular Tweezer with Tunable Intra- and Intermolecular Charge Transfer, *Chem. – Eur. J.*, 2017, **23**, 15012–15016.

29 K. C. Gupta and A. K. Sutar, Catalytic activities of Schiff base transition metal complexes, *Coord. Chem. Rev.*, 2008, **252**, 1420–1450.

30 W. A. Zoubi and Y. G. Ko, Organometallic complexes of Schiff bases: Recent progress in oxidation catalysis, *J. Organomet. Chem.*, 2016, **822**, 173–188.

31 L. John, R. S. Joseyphus and I. H. Joe, Synthesis, characterization and antimicrobial activity of transition metal complexes with the Schiff base derived from imidazole-2-carboxaldehyde and glycylglycine, *J. Coord. Chem.*, 2019, **62**, 319–327.

32 A. Najafian and T. R. Cundari, Effect of Appended S-Block Metal Ion Crown Ethers on Redox Properties and Catalytic Activity of Mn–Nitride Schiff Base Complexes: Methane Activation, *Inorg. Chem.*, 2019, **58**, 12254–12263.

33 Y. Yang, C. Y. Gao, J. L. Liu and D. W. Dong, Recent developments in rhodamine salicylidene hydrazone chemosensors, *Anal. Methods*, 2016, **8**, 2863–2871.

34 C. J. Dhanaraj and J. Johnson, Synthesis, characterization, electrochemical and biological studies on some metal(ɪɪ) Schiff base complexes containing quinoxaline moiety, *Spectrochim. Acta, Part A*, 2013, **118**, 624–631.

35 M. B. Dai, Q. L. Zhang, X. C. Zhu, Y. Q. Zhang and B. X. Zhu, Synthesis and Crystal Structure of Schiff Base Ligand and Dinuclear Cu(ɪɪ) Complex, *Chin. J. Inorg. Chem.*, 2008, **24**, 1381–1386.

36 *36SAINT and APEX 2 software for CCD diffractometers*, Bruker AXS Inc., Madison, USA, 2015.

37 G. M. Sheldrick, SHELXT – Integrated space-group and crystal-structure determination, *Acta Crystallogr.*, 2015, **A71**, 3–8.

38 A. L. Spek, *Acta Crystallogr.*, 2015, **C71**, 9–18.

39 H. Y. Chen, C. Huang, Y. Z. Ding, Q. L. Zhang, B. X. Zhu and X. L. Ni, Organic core–shell-shaped micro/nanoparticles from twisted macrocycles in Schiff base reaction, *Chem. Sci.*, 2019, **10**, 490–496.